



Article

GRACE-Derived Terrestrial Water Storage Changes in the Inter-Basin Region and Its Possible Influencing Factors: A Case Study of the Sichuan Basin, China

Chaolong Yao ^{1,2}, Zhicai Luo ^{1,3,4,5}, Haihong Wang ^{1,*}, Qiong Li ⁶ and Hao Zhou ⁶

¹ School of Geodesy and Geomatics, Wuhan University, Wuhan 430079, Hubei, China; clyao@whu.edu.cn (C.Y.); zhcluo@sgg.whu.edu.cn (Z.L.)

² Guangxi Key Laboratory of Spatial Information and Geomatics, Guilin University of Technology, Guilin 541004, Guangxi, China

³ Key Laboratory of Geospace Environment and Geodesy, Ministry of Education, Wuhan University, Wuhan 430079, Hubei, China

⁴ State Key Laboratory of Information Engineering in Surveying, Mapping and Remote Sensing, Wuhan University, Wuhan 430079, Hubei, China

⁵ Collaborative Innovation Center for Geospatial Technology, Wuhan University, Wuhan 430079, Hubei, China

⁶ MOE Key Laboratory of Fundamental Physical Quantities Measurement, School of Physics, Huazhong University of Science and Technology, Wuhan 430074, Hubei, China; liqiong_dlp@126.com (Q.L.); lengyeshanren@126.com (H.Z.)

* Correspondence: hhwang@sgg.whu.edu.cn; Tel.: +86-27-6877-1756

Academic Editors: Cheinway Hwang, Wenbin Shen, C.K. Shum, Stéphane Calmant, Magaly Koch and Prasad S. Thenkabail

Received: 27 February 2016; Accepted: 19 May 2016; Published: 26 May 2016

Abstract: We investigate terrestrial water storage (TWS) changes over the Sichuan Basin and the related impacts of water variations in the adjacent basins from GRACE (Gravity Recovery and Climate Experiment), *in situ* river level, and precipitation data. Although GRACE shows water increased over the Sichuan Basin from January 2003 to February 2015, two heavy droughts in 2006 and 2011 have resulted in significant water deficits. Correlations of 0.74 and 0.56 were found between TWS and mean river level/precipitation within the Sichuan Basin, respectively, indicating that the Sichuan Basin TWS is influenced by both of the local rainfall and water recharge from the adjacent rivers. Moreover, water sources from the neighboring basins showed different impacts on water deficits observed by GRACE during the two severe droughts in the region. This provides valuable information for regional water management in response to serious dry conditions. Additionally, the Sichuan Basin TWS is shown to be influenced more by the Indian Ocean Dipole (IOD) than the El Niño-Southern Oscillation (ENSO), especially for the January 2003–July 2012 period with a correlation of -0.66 . However, a strong positive correlation of 0.84 was found between TWS and ENSO after August 2012, which is a puzzle that needs further investigation. This study shows that the combination of other hydrological variables can provide beneficial applications of GRACE in inter-basin areas.

Keywords: GRACE; water storage variability; Indian Ocean Dipole; El Niño-Southern Oscillation; Sichuan Basin

1. Introduction

The Sichuan Basin, located in the east of Tibetan Plateau (TP), is an inter-basin region. It belongs mainly to four sub-basins in the upper Yangtze, including the Jinsha River, the Minjiang River, and the Jialing River, originating from the Qinghai-Tibet Plateau, and the Wujiang River in the Yun-Gui

Plateau. The hydrological variations of the Sichuan Basin is influenced by the TP through atmospheric circulation [1] and water interaction with the adjacent rivers originating from the TP [2]. For instance, Tao *et al.*, [3] found the connections between Tibetan weather systems and heavy rains in the Sichuan Basin. As one of the four main basins in China, the Sichuan Basin provides the greatest rice yield and is an important commodity grain base, nationally. Frequent climate extremes, including droughts and floods, as well as intensive human intervention, e.g., water impoundment by dams and irrigation, have been dramatically influencing the hydrological regime over the Yangtze River basin [4–7]. During the past 40 years, the long-term decrease in precipitation and runoff in autumn over the east of the Sichuan Basin [7] and a significant drying trend in the entire Sichuan Basin [8] possibly cause more frequent or extreme droughts. For example, two severe drought events happened in 2006 and 2011, which have posed significant water security concerns in a short-term [4,7,9,10]. Moreover, runoff in the upper Yangtze River basin concentrates on various regions in different seasons [7]. Therefore, the investigation of water variability in the Sichuan Basin and its connections with the possible influencing factors are of importance for drought forecasting, water management, and food security.

Precipitation, river stage (water level), soil moisture, and other hydrological variables have been widely employed to characterize the hydrological cycle worldwide (e.g., [8,11–15]). Particularly, some drought indices based on these hydrological parameters were developed for drought characterization in terms of meteorology and hydrology, such as the Palmer Drought Severity Index (PDSI) [16], the Standardized Precipitation Index (SPI) [17], the streamflow drought index (SDI) [18], and the surface water supply index (SWSI) [19]. These drought monitors have been proven to be valuable tools for drought assessment. Recently, several drought indices were applied to assess the droughts in the Sichuan Basin and its surrounding areas [9,20]. Nevertheless, precipitation with high spatial variability provides insufficient information for studies at the river basin scale [21]. River level variations are sensitive to the local precipitation [21], and may largely be affected by non-climatic factors such as reservoir impounding and irrigation [10,22]. Since hydrological variables show different features in response to a drought processes [23,24], a lack of information on groundwater makes these drought characterization frameworks uncomprehensive.

Since 2002, terrestrial water storage (TWS) measured by the GRACE (Gravity Recovery and Climate Experiment) space gravimetry mission has become a valuable parameter for studying the water balance over large-scale regions with monthly time resolution [25–27]. Many studies have used GRACE-based TWS, along with other hydrological components to characterize water variations over various regions, and their correlations with climate variability have also been highlighted. Examples include the Amazon basin [21], the Yangtze River basin [10], the Nile basin [28], and the East African Great Lakes region [29]. These studies indicate that the combination with other data sources could maximize the benefit of GRACE data. Furthermore, GRACE shows great potential for monitoring droughts comprehensively, e.g., [30–32], as it provides vertically-integrated water storage variations, including changes in surface water, soil moisture, and groundwater, while these water components are not accessible from direct measurements simultaneously so far.

In this study, we examine the TWS change over the Sichuan Basin from GRACE. Its correlations with river level/precipitation data in the adjacent basins are also analyzed. We investigate the river level and precipitation data in the four main streams (see Figure 1 for location), which directly impact the TWS changes over the Sichuan Basin. This allows us to find their influences on TWS during the 2006 and 2011 droughts, and would be valuable for regional water management. Possible teleconnections between the Sichuan Basin TWS and Indo-Pacific climate variability are also assessed using indices of the Indian Ocean Dipole (IOD), El Niño-Southern Oscillation (ENSO), and Pacific Decadal Oscillation (PDO).

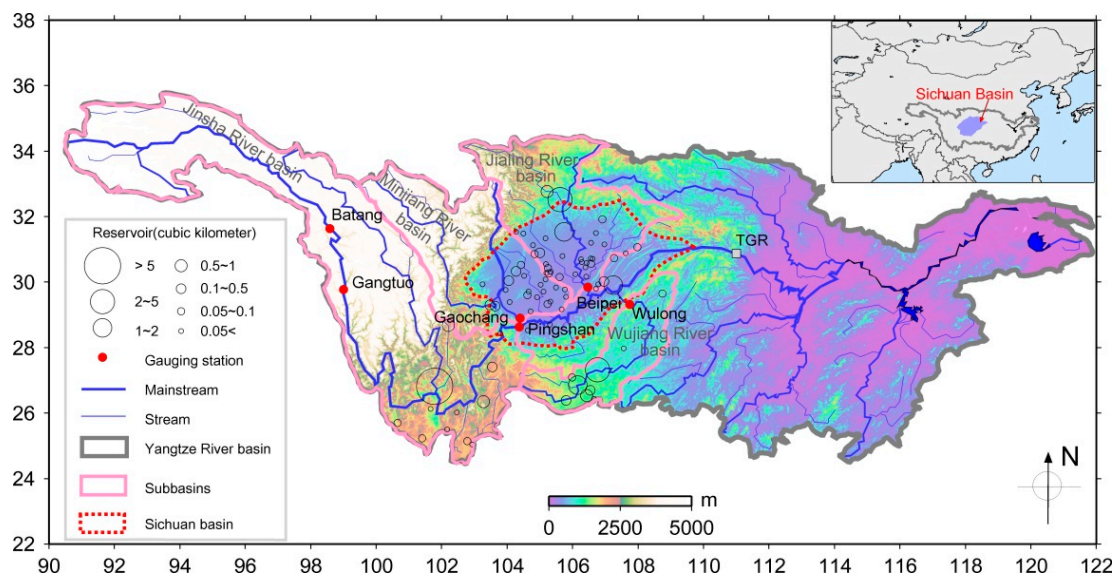


Figure 1. Yangtze River basin and its main sub-basins in the upper reach. The circle represents the location and capacity of reservoirs.

2. Study Region

The Sichuan Basin can be divided into two parts: the mountainous area and the plain area. The study area focuses on the plain region subjected to intensive surface water irrigation, with an area of 197,330 km² and the elevation varying from 200 m up to 750 m. Irrigated areas with surface water accounts for more than 90% in the Sichuan Basin [4]. Many dams have been built for agricultural irrigation [33] (Figure 1). The hydrological regime of the study area is influenced directly by the four sub-basins in the upper Yangtze River. Most of dams were built in the Jialing River and Minjiang River basins (Figure 1).

Among the four sub-basins, the Jialing River basin is the largest one in the upper Yangtze River. The Wujiang River basin is formed primarily by a karst geological environment, with a runoff coefficient of 0.531 [34]. The Jinsha River originates from the Batang River estuary in the Qinghai-Tibet Plateau and ends in the Sichuan Province. Its elevation difference can reach 1000–3000 m, and the high annual streamflow of 149.8 billion km³ in its lower section [2] is an important water source for the Sichuan Basin. The Minjiang River basin has the largest mean discharge in the upper Yangtze River, and it plays a crucial role for the Chengdu Plain in terms of economy and environment [35].

3. Data and Methods

3.1. GRACE Data

GRACE, a satellite project jointly sponsored by NASA and the German Aerospace Center, was launched in March 2002. Its primary scientific object is to accurately detect variations in the Earth's gravity field. Currently, spatial-temporal change of the Earth's gravity field can be measured with a resolution of about 300 km or better by using reprocessed GRACE solutions [36]. Such time-variable gravity fields provide information on mass variations in the surface of the Earth, e.g., snow, surface water, ocean, continental ice sheets, and mountain glaciers [37]. In particular, GRACE-sensed TWS changes have been widely used for a range of hydrological applications.

In this study, monthly gravity fields from RL05 (at degree and order 60) provided by the Center for Space Research (CSR) at the University of Texas at Austin and RL05a (at degree and order 90) provided by the German Research Center for Geoscience (GFZ) for the period of January 2003 to February 2015 were used to calculate TWS changes. Anomalous gravity fields were obtained by removing the mean

field with respect to the study period. Data were processed following the methods of Luo *et al.* [38], including: (1) degree-2 zonal C20 time series were replaced by analyzed Satellite Laser Ranging (SLR) data [39]; and (2) a hybrid filtering scheme combined de-correlation filter P3M6 (at spherical harmonic orders 6 and above, a three order polynomial is fitted by least squares and is removed from even and odd coefficient pairs) [40] and 300 km Fan filter [41] was applied to reduce noise from GRACE data.

To restore the possible signal attenuation in GRACE, we processed the soil moisture (SM) data from the Global Land Data Assimilation System (GLDAS)/Noah land surface model [42] in the same way as GRACE data (e.g., truncation, destriping, and smoothing). The grid scaling factors were then obtained by least squares fit between the smoothed and the original SM signals from GLDAS. Due to the warm climate and the shallow terrain, snow is uncommon in the study region. The monthly snow water equivalent (SWE) calculated from four models (CLM, MOSAIC, NOAH, VIC) in GLDAS-1 is generally less than 0.5 mm. Therefore, we did not consider its contribution in estimating scaling factors. Consequently, the regional scaling factors are 1.44 for CSR and 1.45 for GFZ, which is slightly larger than the value of 1.23 derived from CLM 4.0 provided by the GRACE Tellus website [43] for the same region.

3.2. Water Level, Precipitation and Temperature Data

Daily water level measurements at six gauging stations (Table 1) were used in our analysis. Three stations such as Batang, Gangtuo, and Pingshan locate in the Jinsha River basin, which is also the mainstream of the Yangtze River. The last four stations in Table 1 are set at the outlet of the four sub-basins, respectively. Therefore, the water level of these four stations can be approximately regarded as an indicator of water variations in its corresponding sub-basin. For consistent with GRACE, the river level data were converted to monthly time scale. Monthly gridded precipitation data from 2000 to February 2015 and temperature data from 2003 to 2013 with the same spatial resolution of $0.5^\circ \times 0.5^\circ$ provided by the China Meteorological Administration (CMA) [44] were used for investigating the meteorological forcing of TWS changes in the Sichuan Basin.

Table 1. Description of the gauging stations and time span of available data.

Gauges	Location	Catchment Area (km ²)	Time Period
Batang	Mainstream	149,072	2000–2013
Gangtuo	Mainstream	180,055	2000–2013
Pingshan	Mainstream	458,592	2000–2012
Gaochang	Outlet of the Minjiang River	135,378	2000–2013
Beipei	Outlet of the Jialing River	156,736	2000–2013
Wulong	Outlet of the Wujiang River	83,035	2000–2013

3.3. ENSO, IOD and PDO

Recent studies have shown that GRACE TWS change is closely linked to ENSO events in parts of the world where precipitation largely dominate regional TWS anomalies e.g., [10,21,29,36,45,46]. Particularly, the precipitation and TWS over the Yangtze River basin are influenced by the sea surface temperature (SST) anomalies of the Pacific Ocean (East Asian monsoon) [10,47–50] and the Indian Ocean (South Asian monsoon) [48,50,51].

We used the IOD which represents the gradient (named as DMI, dipole mode index) in SST anomaly between the tropical western Indian Ocean (50°E – 70°E , 10°S – 10°N) and the tropical South-eastern Indian Ocean (90°E – 110°E , 10°S –equator) [52] to analyze the relation between the Sichuan Basin TWS and the Indian monsoon. The IOD was first identified in 1999 and affects many nations' climate around the Indian Ocean rim [53–57]. The ENSO index is represented by the Niño 3.4 provided by the Climate Prediction Centre (CPC). It represents a mean SST anomaly in the region between 5°N – 5°S and 170°W – 120°W . The PDO provided by the Joint Institute for the Study of the Atmosphere and Ocean (JISAO) is a largely interdecadal oscillation, which can modulate the

interannual ENSO-related teleconnections [58]. The impacts of ENSO in association with PDO on precipitation and streamflow have been found in eastern Australia, South America, and China [58–60].

4. Results

4.1. Comparisons of TWS, SM and Precipitation Changes

Figure 2 shows the spatial long-term trend distribution of TWS, SM, and precipitation. Apparent increased water over the Sichuan Basin can be seen from GRACE solutions for the study period, coinciding with prior work by Zhao *et al.* [61]. The increasing trend can be observed in 65% area of the basin from the GLDAS SM. The significant decreasing trend in SM (Figure 2c) near Gaochang, where the precipitation (Figure 2d) shows a slight increase, might result from the uncertainty of the GLDAS model. The increased water could be explained by the increase in precipitation within the Sichuan Basin and over the upper Jialing River and Minjiang River basins (Figure 2d). In particular, all data show significant increased trends in the Chengdu Plain (around the Chengdu City, with an area of $\sim 10,000$ km²).

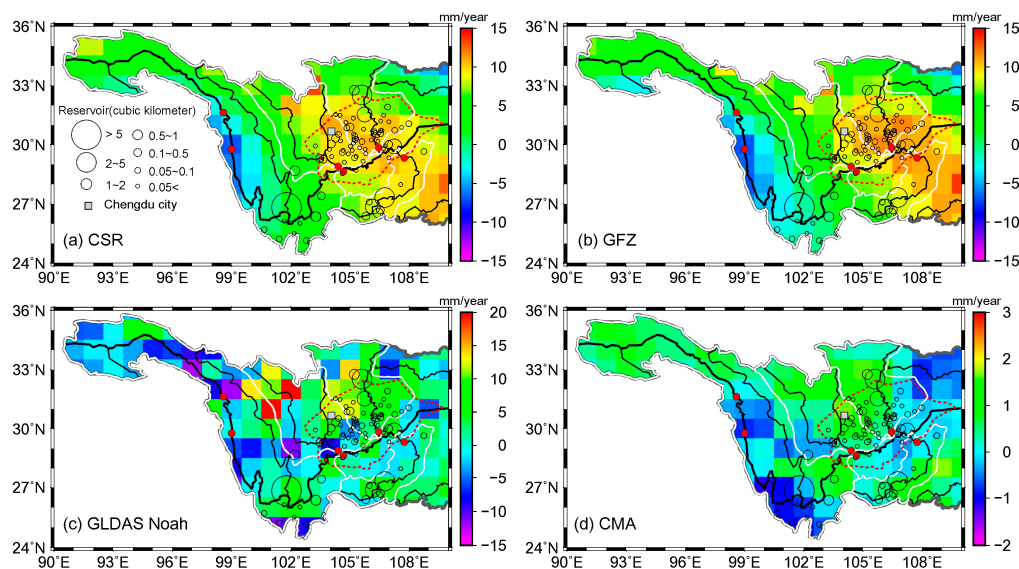


Figure 2. Linear trend variability of changes in: (a) CSR TWS; (b) GFZ TWS; (c) GLDAS Noah SM; and (d) CMA precipitation for the period of January 2003 to February 2015. Note that precipitation data have been resampled in a $1^\circ \times 1^\circ$ grid for a reliable comparison.

Some large discrepancies between SM and precipitation could be expected to occur in regions where artificial water impoundment dominate TWS, such as around the Ertan reservoir with a capacity of 5.8 km³ in the lower Jinsha River and the upper Wujiang River (Figure 2c,d). Previous study also showed that large dams have greatly impacted the seasonal and monthly river discharge for some tributaries in the upper Yangtze [7]. Obvious discrepancies between TWS and SM/precipitation along the southeast boundary of the study region could be attributed to the strong signal leakage at the transition between the plains and the mountain areas, where the TWS signal generally contains strong gradients in phase [62]. Additionally, GRACE cannot detect the obvious decreasing trend signal in SM and precipitation over the lower reach of the Minjiang River mainly due to its lower spatial resolution.

Long-term increasing trends in regional TWS and SM for the period January 2003 to February 2015 can be seen from Figure 3a, and they generally agree well in both of amplitude and timing. The trends of CSR and GFZ are very close, with rates of 6.4 ± 1.0 mm/year and 6.6 ± 1.1 mm/year respectively, which are larger than the value of 2.6 ± 0.8 mm/year for GLDAS. This implies that other water components, such as surface water and groundwater, contributed to more than half of the increased

water in the Sichuan Basin during the study period. Although increasing trends are shown over most Sichuan Basin (Figure 2), two extremely low TWS and SM occurred in 2006 and 2011, consistent with the persistent low precipitation from the time series of the three-month mean precipitation (Figure 3). During these two dry periods, the annual mean precipitation in 2006 (71 mm) and 2011 (78 mm) are 18.4% and 10.3% lower than the mean value (87 mm) for the whole study period, respectively, and the precipitation deficits mainly concentrated on summer (Figure 4). This demonstrates that the 2006 drought is more severe than the 2011 drought. Moreover, the highest temperature of 28.3 °C for the 2003–2013 period occurred in August 2006 (Figure 3b). This resulted in increased evapotranspiration, and subsequently caused an extra water loss from soil and surface water bodies in the Sichuan Basin. A significant low TWS was observed in 2003. However, this signal was arguable because of large discrepancy between TWS and SM, which will be discussed in Section 4.2.

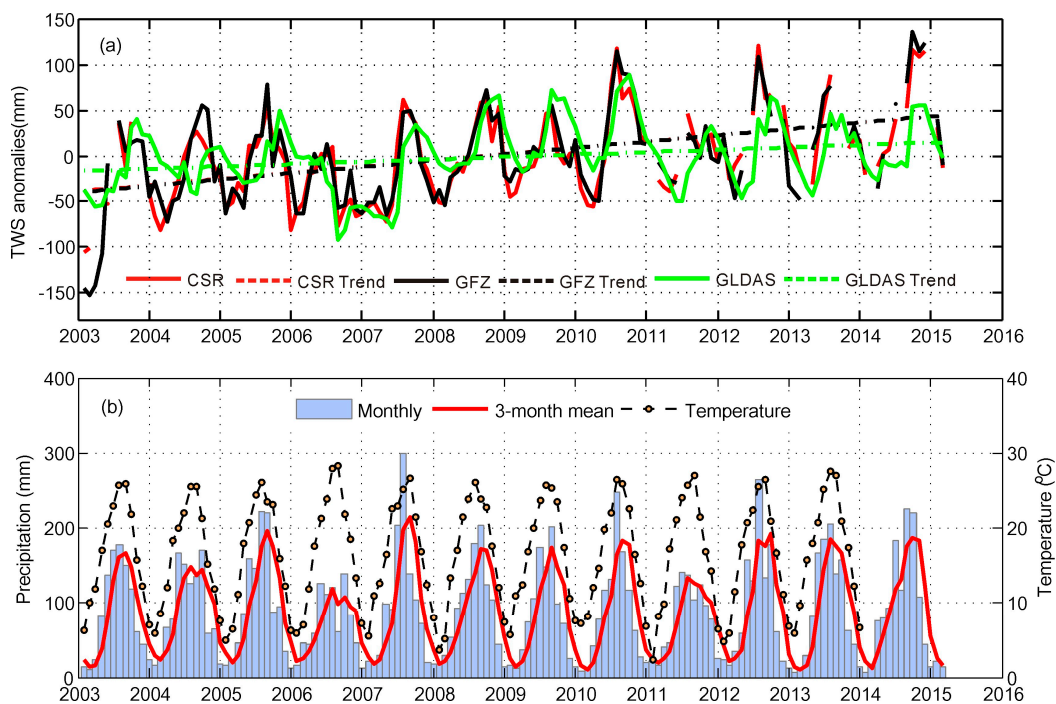


Figure 3. Time series of (a) monthly water storage variations from CSR, GFZ, and GLDAS; and (b) monthly precipitation and temperature, and three-month mean precipitation.

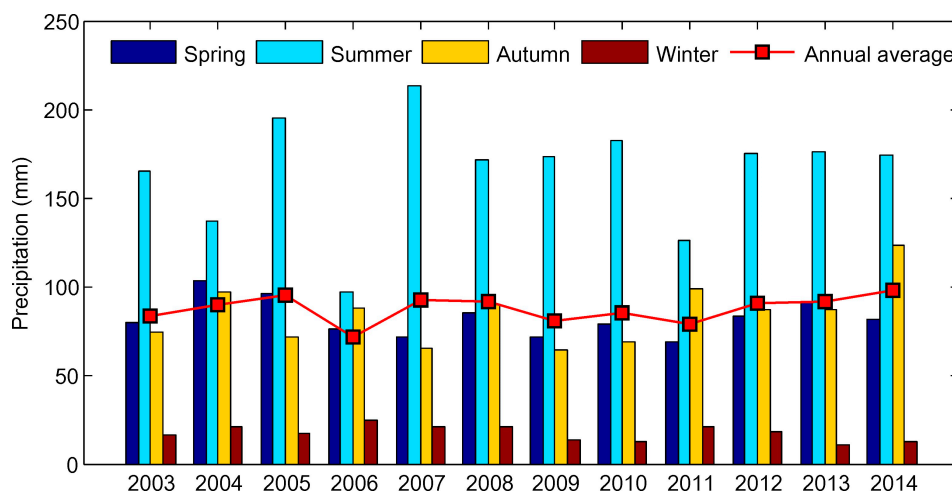


Figure 4. Seasonal and annual average precipitation in the Sichuan Basin.

4.2. Correlation between the Sichuan Basin TWS and River Level

The seasonal variation and linear trend were removed from the original signals of TWS, river level, and precipitation to obtain the non-seasonal anomalies, which can reflect the non-seasonal anomalous conditions of droughts and floods. Then, a five-month moving window was applied to the time series of these non-seasonal anomalies. The TWS variations in the Sichuan Basin shown in Figures 5–7 are the mean of CSR and GFZ. For the missing values in GRACE TWS, interpolation was simply performed by averaging the values before and after the missing data. The mean river level shown in Figure 5 is the average of the measurements at four gauging stations (Pingshan, Gaochang, Beipei and Wulong) within the Sichuan Basin.

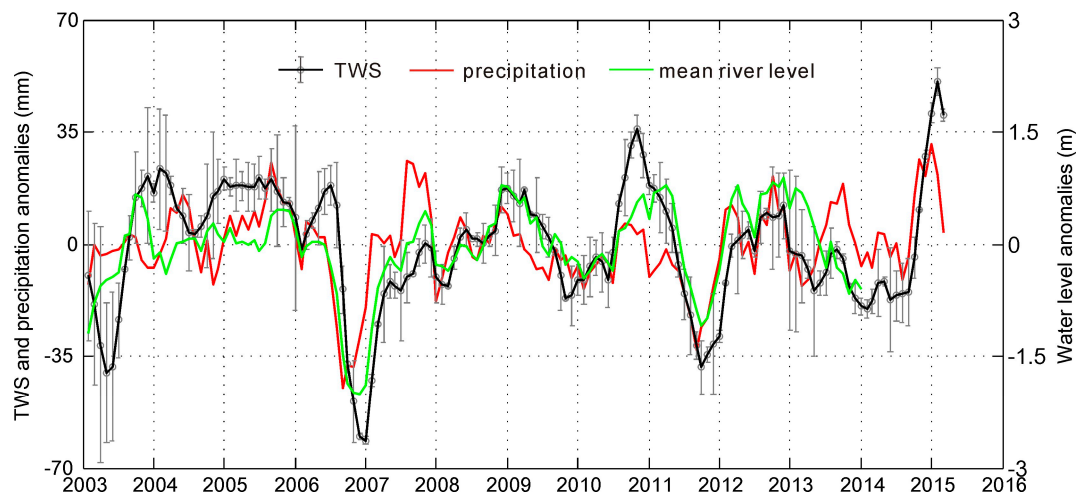


Figure 5. Time series of non-seasonal variations in TWS, mean river level and precipitation within the Sichuan Basin. The error bars show the uncertainties of GRACE data, represented by the standard deviation of non-seasonal TWS difference between CSR and GFZ solutions.

Figure 5 shows the behaviors of non-seasonal changes in TWS, mean river level and precipitation within the Sichuan Basin. Before the 2006 drought, there was a long-term positive TWS anomaly in 2005, consistent with river level and precipitation data. Significant precipitation deficits caused severe water depletions in 2006 and 2011, corresponding to the heavy droughts in the upper Yangtze. Differently, TWS increased to ‘normal’ in a relative short time period after the 2011 drought event responding to the recovery of precipitation. While there was a continuous below-average TWS and river level after the 2006 heavy drought despite of positive anomalies in precipitation. Subsequently, after the water increase following the 2011 drought, a long-term negative TWS anomaly lasted from January 2013 to October 2014, which showed a complex response pattern to the precipitation and river level. The complex pattern might be related to the regulation of reservoir operation in the upper Yangtze River. It was reported that the number of reservoirs involved into unified regulation by the government increased from 10 in 2012 to 17 in 2013 [63].

In 2003, GRACE also measured large water depletions with the magnitude close to that of the drought event in 2011. The strong negative anomalies of the mean river level in early 2003 seemed to agree with the water depletion. However, no significant anomaly occurred in the SM (Figure 3a) and precipitation (Figure 5). Considering the large uncertainties of the TWS as well (Figure 5), caused by the relative poor quality of GRACE observations at its early stage [10,45], it is difficult to confirm whether the water depletions in 2003 resulted from hydrological effects. More independent hydrological variables are needed to verify this large anomaly in GRACE-derived TWS.

As an inter-basin region, the mean river level variations within the Sichuan Basin partially reflect water variability in the neighboring basins, because the gauge stations are located at the outlet of these basins. Correlation coefficients of 0.74 and 0.56 were found between TWS and mean river

level/precipitation data, respectively, indicating that the Sichuan Basin TWS is influenced not only by the local rainfall, but also impacted by water variations in the adjacent basins. Particularly, water sources from the adjacent rivers predominated on TWS in some periods. For instance, negative precipitation anomalies in late 2003 and in early 2011 correspond to increased TWS. This could be attributed to a significant water recharge from the adjacent rivers as river level anomalies were obviously positive at the same time periods. Similar cases can be found in late 2004 and early 2009. Another contrary example occurred in mid-2013. In this case, the precipitation was significantly above normal, while TWS and river level anomalies were negative.

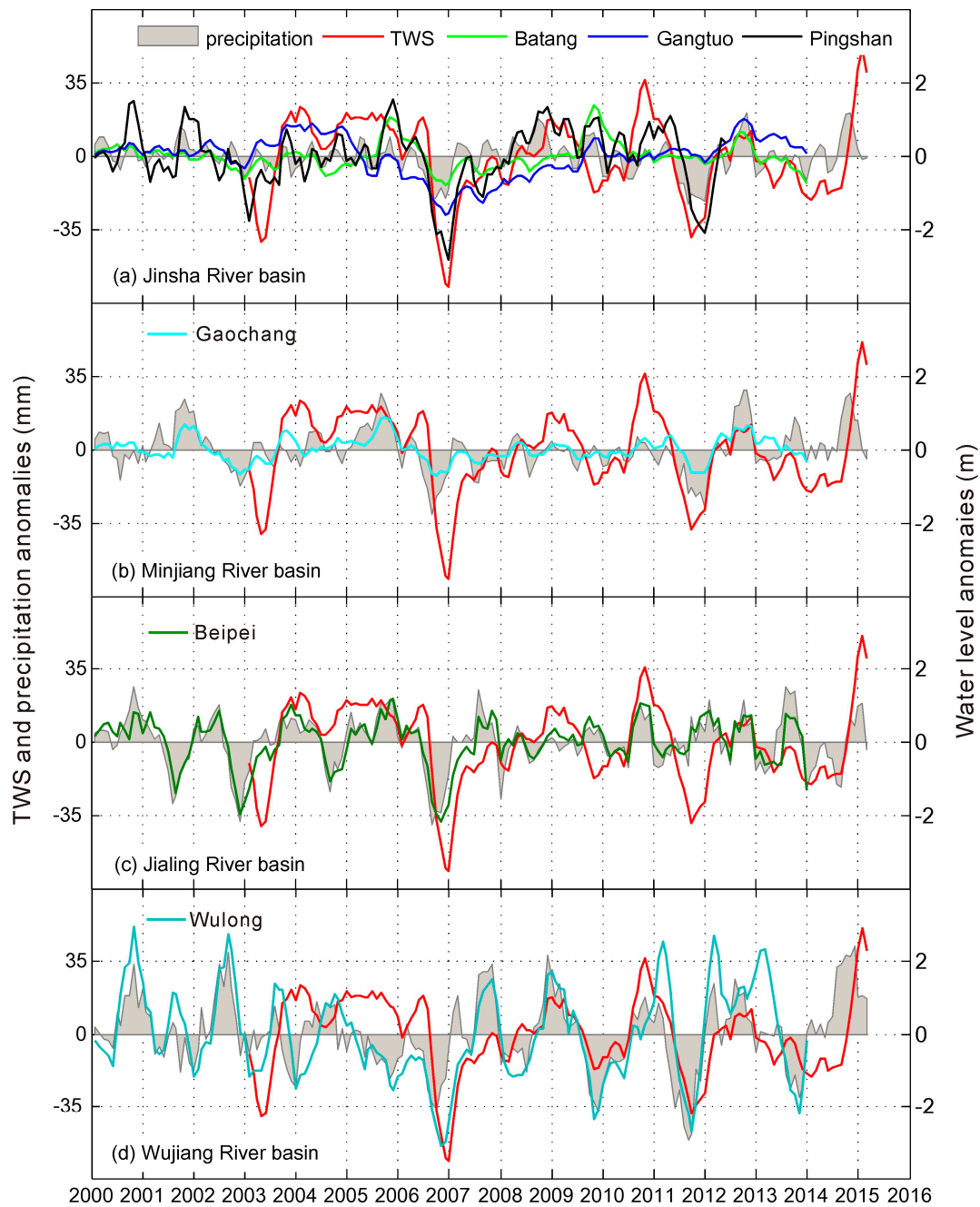


Figure 6. Time series of non-seasonal anomalies in the Sichuan Basin TWS, and river level/precipitation in the (a) Jinsha River basin; (b) Mijiang River basin; (c) Jialing River basin; and (d) Wujiang River basin.

Correlations between the Sichuan Basin TWS and river level at the six gauging stations were further investigated to find the related impacts of water variations in each basin (Figure 6). River levels at Pingshan and Gaochang behaved with higher correlations with TWS than those at other stations, with the same correlation coefficient of 0.68. It is surprising that the correlation coefficient between levels at Beipei and TWS is only 0.54, although the Sichuan Basin includes most areas of the Jialing River basin. This implies that the Sichuan Basin TWS could be influenced by other factors, e.g., water recharge from other neighboring river basins and damming effects in the upper Jialing River. Actually, the Wujiang River basin is not located in the study area, but it disembogues into the Sichuan Basin through Wulong station. The river level variations at Wulong station correspondingly display a relative weak correlation (0.46) with the water variability of Sichuan Basin. However, the significant water deficits observed by GRACE in 2006, late 2009, and 2011 are consistent with obvious negative river level anomalies (Figure 6d). Correlations between TWS and river level at Batang and Gangtuo stations are 0.34 and 0.28, respectively, which are much less than other stations. The reason is that their locations cannot represent the entire Jinsha River basin.

The impacts of the four sub-basins in the upper Yangtze River for the 2006 and 2011 drought events in the Sichuan Basin are different. In 2006, extreme low anomalies were recorded at all stations, and the river level at three stations (Pingshan, Beipei, and Wulong) decreased by more than 2 m. This demonstrates that consistent negative impacts from the four sub-basins contributed to the exceptional drought event. However, obvious negative impacts on the 2011 drought were from the Jinsha River and the Wujiang River. Remarkably, the contribution from the Jinsha River concentrated on its lower reach, since the river level at Batang and Gangtuo stations kept normal in 2011. Previous work by Tang *et al.* [50] also showed significant water depletions in the lower Jinsha River due to recent heavy droughts in Southwest China. In contrast, the Jialing River exerted a positive impact on this event, which was quite different from the other rivers.

4.3. The Sichuan Basin TWS and Climate Variability

Zhang *et al.* [10] showed that a normalized GRACE-based TWS could be a valuable hydro-climatological index in the Yangtze River basin. In order to better understand the relationship between the Sichuan Basin and climate variability, the time series of climate indices, non-seasonal TWS, and precipitation anomalies were normalized (Figure 7). In general, the upper Yangtze would be expected to be dry in El Niño and wet in La Niña [10]. Similar results can be seen in the Sichuan Basin, such as the dry conditions around 2006 and 2010, and a wet episode in 2010 (Figure 7a). This is, however, not the case in the 2011 drought, with a dry condition in the 2011–2012 La Niña. The significant TWS/precipitation absents during 2011–2012 could, therefore, be attributed to other factors such as IOD, given that this water depletion is coincident with a positive IOD phase (Figure 7b). Tang *et al.* [50] also suggested that the persistent warm phase in the southern Indian Ocean is likely to cause the 2010–2011 heavy drought in Southwestern China. Similar cases have been found in the Blue Nile in Africa as well, that IOD exerted influence on regional precipitation in 1997 and 2006–2007 ENSO year [28,64].

The Sichuan Basin TWS is more closely related to IOD than ENSO since a negative correlation of -0.48 between TWS and IOD was obtained, as opposed to insignificant correlation between TWS and ENSO for the study period (Table 2). From Figure 7b, a long-term positive TWS anomaly from 2004 to the mid-2006 is consistent with negative IOD anomalies. Two serious dry conditions around 2006 and 2011 and a significant wet episode in late 2010 are well correlated with IOD events as well. Zhang *et al.* [10] also pointed out that the TWS in the upper Yangtze in Southwest China seems to be more influenced by the Indian monsoon. Furthermore, the significant intensification of Rossby waves during the co-occurrence of positive IOD and El Niño also affects the Tropical Indian Ocean climate [65], and therefore influences the Asian climate. This may explain a small El Niño event in 2006 corresponds to a serious water deficit. In addition, positive TWS/precipitation anomalies from

mid-2007 to late 2009 and 2010–2011 agree well with the cool PDO-La Niña phase, coinciding with the finding in Ouyang *et al.* [58].

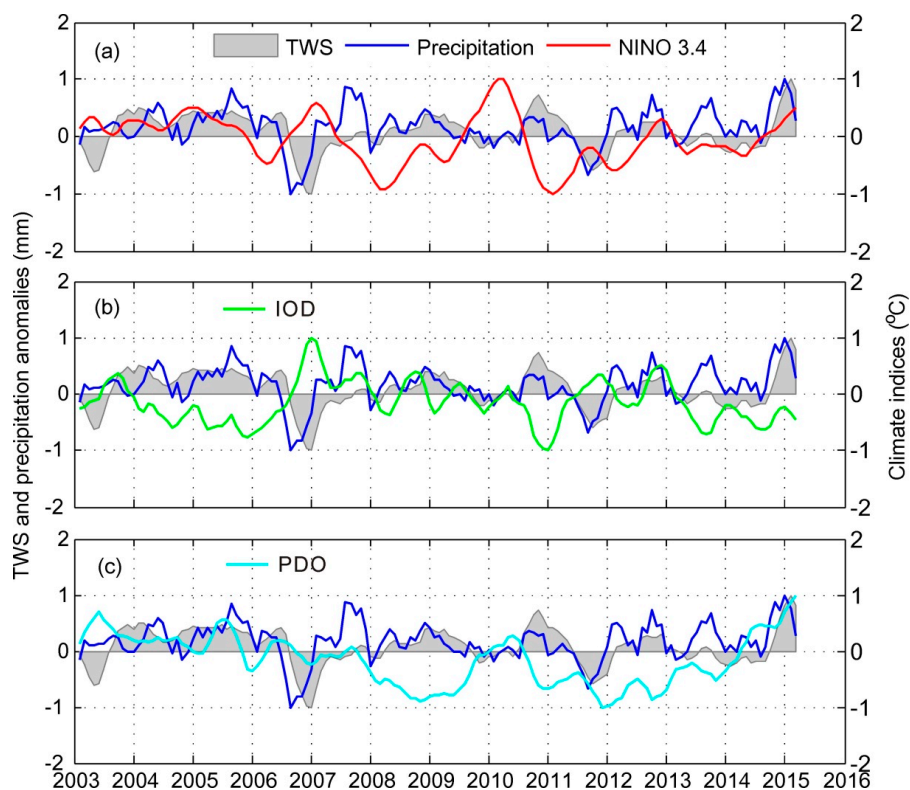


Figure 7. Normalized and five-month mean time series of non-seasonal Sichuan Basin TWS anomalies, precipitation, and indices of (a) NINO 3.4; (b) IOD; and (c) PDO.

Table 2. Correlation coefficients between TWS/precipitation and IOD/ENSO over the Sichuan Basin. The insignificant values are marked in bold. Correlations are computed at 95% level of confidence.

	IOD/ENSO		
	January 2003–February 2015	January 2003–July 2012	August 2012–February 2015
TWS	−0.48/−0.08	−0.66/−0.20	0.20/0.84
precipitation	−0.24/−0.02	−0.25/−0.09	0.03/0.47

Additionally, opposite correlations before and after July 2012 were found between TWS/precipitation and IOD/ENSO. Before July 2012, the TWS is negatively correlated with IOD with a correlation of -0.66 , whereas a strong positive correlation of 0.84 was found between TWS and ENSO after this time (Table 2). This change happened after two continued La Niña events in 2011–2012, as well as in a long-term significant cool PDO phase, and may have imposed various climate extremes in many regions [66]. A similar mechanism was also found in southern China that the rainfall-ENSO relationship changed in different periods, which is likely related to SST anomalies in Indian Ocean and the modulation of the PDO [67,68]. Additionally, the sensible heat over the TP affects the timing and the onset of the East Asian summer monsoon [69], in particular the weakening of the sensible heat [9] may influence the suppressed Asian monsoon [70] to some degree. Since complex effects on the hydrological variations over the Yangtze River have been noticed, e.g., [10,71], a combination of climatic systems influence such as the contribution from the local land surface processes and the remote TP heating, polar ice coverage and Eurasian snow cover [10,58,72,73] are necessary for a complete analysis.

5. Conclusions

In the present study, we have investigated the spatio-temporal variability of TWS over the Sichuan Basin and the related impacts of water sources from the adjacent basins using GRACE space gravimetry, river level, and precipitation data. GRACE shows water increased over the Sichuan Basin between January 2003 and February 2015, which is caused largely by the increased precipitation. Two severe drought events in 2006 and 2011 were observed from GRACE-derived TWS, river level, and precipitation data. Composite analysis based on GRACE and hydro-meteorological data demonstrate that the adjacent four river basins have different influences on the Sichuan Basin TWS. This study indicates, once again, that GRACE provides an alternative and independent way to quantify hydrological extremes, and a combination with other hydrological parameters could be beneficial for GRACE applications in inter-basin or inter-aquifer areas.

The Sichuan Basin TWS variation is influenced by both of IOD and ENSO for the whole study period. During the period of January 2003–July 2012, IOD behaved stronger negative correlation with TWS than ENSO. However, the case was changed after August 2012, which might result from the modulation of PDO. Correlations between TWS and IOD/ENSO became positive and the influence of ENSO overtook IOD. The evidence shown in this study, along with previous results may contribute to the investigation of the mechanism of climate impacts on the Sichuan Basin, and a comprehensive analysis would incorporate the local and remote effects.

Acknowledgments: We would like to thank the reviewers for their highly insightful comments, which enable us to greatly improve the quality of our manuscript. We are grateful to CSR at the University of Texas at Austin and GFZ for providing the GRACE monthly gravity field models and GSFC/NASA for providing LSMs data in GLDAS-1. This work was supported by the National Natural Science Foundation of China (Grant Nos. 41174020, 41131067, 41429401, 41174021), the National Basic Research Program of China (973 Program) (Grant No. 2013CB733302), the Fundamental Research Funds for the Central Universities (Grant No. 2014214020203), the open fund of Key Laboratory of Geospace Environment and Geodesy, Ministry of Education (Grant No. 14-02-011) and the open fund of Guangxi Key Laboratory of Spatial Information and Geomatics (Grant No. 14-045-24-17).

Author Contributions: Chaolong Yao, Zhicai Luo and Haihong Wang conceived of this study; Chaolong Yao, Qiong Li and Hao Zhou collected the data and conducted the experiments; Chaolong Yao and Haihong Wang analyzed the data. All authors contributed to writing the paper.

Conflicts of Interest: The authors declare no conflict of interest.

References

1. Duan, A.; Wu, G. Weakening trend in the atmospheric heat source over the Tibetan Plateau during recent decades. Part I: Observations. *J. Clim.* **2008**, *21*, 3149–3164. [[CrossRef](#)]
2. Song, M.-B.; Li, T.-X.; Chen, J.Q. Preliminary analysis of precipitation-runoff features in the Jinsha River Basin. *Procedia Eng.* **2012**, *28*, 688–695.
3. Tao, S.-Y.; Ding, Y.-H. Observational evidence of the influence of the Qinghai-Xizang (Tibet) Plateau on the occurrence of heavy rain and severe convective storms in China. *Bull. Am. Meteorol. Soc.* **1981**, *62*, 23–30. [[CrossRef](#)]
4. Long, D.; Yang, Y.; Wada, Y.; Hong, Y.; Liang, W.; Chen, Y.; Yong, B.; Hou, A.; Wei, J.; Chen, L. Deriving scaling factors using a global hydrological model to restore GRACE total water storage changes for China's Yangtze River Basin. *Remote Sens. Environ.* **2015**, *168*, 177–193. [[CrossRef](#)]
5. Huang, Y.; Salama, M.; Krol, M.S.; Su, Z.; Hoekstra, A.Y.; Zeng, Y.; Zhou, Y. Estimation of human-induced changes in terrestrial water storage through integration of GRACE satellite detection and hydrological modeling: A case study of the Yangtze River basin. *Water Resour. Res.* **2015**, *51*, 8494–8516. [[CrossRef](#)]
6. Chen, X.; Zong, Y.; Zhang, E.; Xu, J.; Li, S. Human impacts on the Changjiang (Yangtze) River basin, China, with special reference to the impacts on the dry season water discharges into the sea. *Geomorphology* **2001**, *41*, 111–123. [[CrossRef](#)]
7. Xu, J.; Yang, D.; Yi, Y.; Lei, Z.; Chen, J.; Yang, W. Spatial and temporal variation of runoff in the Yangtze River basin during the past 40 years. *Quat. Int.* **2008**, *186*, 32–42. [[CrossRef](#)]
8. Xu, K.; Yang, D.; Yang, H.; Li, Z.; Qin, Y.; Shen, Y. Spatio-temporal variation of drought in China during 1961–2012: A climatic perspective. *J. Hydrol.* **2015**, *526*, 253–264. [[CrossRef](#)]

9. Zhang, W.; Lu, Q.; Gao, Z.; Peng, J. Response of remotely sensed normalized difference water deviation index to the 2006 drought of eastern Sichuan Basin. *Sci. China Earth Sci.* **2008**, *51*, 748–758. [[CrossRef](#)]
10. Zhang, Z.; Chao, B.; Chen, J.; Wilson, C. Terrestrial water storage anomalies of Yangtze River Basin droughts observed by GRACE and connections with ENSO. *Glob. Planet. Chang.* **2015**, *126*, 35–45. [[CrossRef](#)]
11. Zhai, P.; Zhang, X.; Wan, H.; Pan, X. Trends in total precipitation and frequency of daily precipitation extremes over China. *J. Clim.* **2005**, *18*, 1096–1108. [[CrossRef](#)]
12. Wang, A.; Lettenmaier, D.P.; Sheffield, J. Soil moisture drought in China, 1950–2006. *J. Clim.* **2011**, *24*, 3257–3271. [[CrossRef](#)]
13. Groisman, P.Y.; Knight, R.W.; Karl, T.R. Heavy precipitation and high streamflow in the contiguous United States: Trends in the twentieth century. *Bull. Am. Meteorol. Soc.* **2001**, *82*, 219–246. [[CrossRef](#)]
14. Alexander, L.; Zhang, X.; Peterson, T.; Caesar, J.; Gleason, B.; Klein Tank, A.; Haylock, M.; Collins, D.; Trewin, B.; Rahimzadeh, F. Global observed changes in daily climate extremes of temperature and precipitation. *J. Geophys. Res.* **2006**, *111*. [[CrossRef](#)]
15. Koster, R.D.; Dirmeyer, P.A.; Guo, Z.; Bonan, G.; Chan, E.; Cox, P.; Gordon, C.; Kanae, S.; Kowalczyk, E.; Lawrence, D. Regions of strong coupling between soil moisture and precipitation. *Science* **2004**, *305*, 1138–1140. [[CrossRef](#)] [[PubMed](#)]
16. Dai, A.; Trenberth, K.E.; Qian, T. A global dataset of Palmer Drought Severity Index for 1870–2002: Relationship with soil moisture and effects of surface warming. *J. Hydrometeorol.* **2004**, *5*, 1117–1130. [[CrossRef](#)]
17. McKee, T.B.; Doesken, N.J.; Kleist, J. Drought monitoring with multiple time scales. In Proceedings of the Ninth Conference on Applied Climatology, Dallas, TX, USA, 15–20 January 1995; pp. 233–236.
18. Nalbantis, I.; Tsakiris, G. Assessment of hydrological drought revisited. *Water Resour. Manag.* **2009**, *23*, 881–897. [[CrossRef](#)]
19. Shafer, B.; Dezman, L. Development of a surface water supply index (SWSI) to assess the severity of drought conditions in snowpack runoff areas. In Proceedings of the Western Snow Conference, Reno, NV, USA, 19–23 April 1982; pp. 164–175.
20. Zeng, X.; Zhao, N.; Sun, H.; Ye, L.; Zhai, J. Changes and relationships of climatic and hydrological droughts in the Jialing River Basin, China. *PLoS ONE* **2015**, *10*, e0141648. [[CrossRef](#)] [[PubMed](#)]
21. Xavier, L.; Becker, M.; Cazenave, A.; Longuevergne, L.; Llovel, W.; Rotunno Filho, O.C. Interannual variability in water storage over 2003–2008 in the Amazon basin from GRACE space gravimetry, *in situ* river level and precipitation data. *Remote Sens. Environ.* **2010**, *114*, 1629–1637. [[CrossRef](#)]
22. Dai, A.; Qian, T.; Trenberth, K.E.; Milliman, J.D. Changes in continental freshwater discharge from 1948 to 2004. *J. Clim.* **2009**, *22*, 2773–2792. [[CrossRef](#)]
23. AghaKouchak, A.; Farahmand, A.; Melton, F.; Teixeira, J.; Anderson, M.; Wardlow, B.; Hain, C. Remote sensing of drought: Progress, challenges and opportunities. *Rev. Geophys.* **2015**, *53*, 452–480. [[CrossRef](#)]
24. Van Loon, A.F. Hydrological drought explained. *Wiley Interdiscip. Rev. Water* **2015**, *2*, 359–392. [[CrossRef](#)]
25. Ramillien, G.; Famiglietti, J.S.; Wahr, J. Detection of continental hydrology and glaciology signals from GRACE: A review. *Surv. Geophys.* **2008**, *29*, 361–374. [[CrossRef](#)]
26. Wouters, B.; Bonin, J.; Chambers, D.; Riva, R.; Sasgen, I.; Wahr, J. GRACE, time-varying gravity, Earth system dynamics and climate change. *Rep. Prog. Phys.* **2014**, *77*, 116801. [[CrossRef](#)] [[PubMed](#)]
27. Famiglietti, J.S.; Rodell, M. Water in the balance. *Science* **2013**, *340*, 1300–1301. [[CrossRef](#)] [[PubMed](#)]
28. Awange, J.; Forootan, E.; Kuhn, M.; Kusche, J.; Heck, B. Water storage changes and climate variability within the Nile Basin between 2002 and 2011. *Adv. Water Resour.* **2014**, *73*, 1–15. [[CrossRef](#)]
29. Becker, M.; Llovel, W.; Cazenave, A.; Güntner, A.; Crétaux, J.-F. Recent hydrological behavior of the East African Great Lakes region inferred from GRACE, satellite altimetry and rainfall observations. *C. R. Geosci.* **2010**, *342*, 223–233. [[CrossRef](#)]
30. Cao, Y.; Nan, Z.; Cheng, G. GRACE gravity satellite observations of terrestrial water storage changes for drought characterization in the arid land of Northwestern China. *Remote Sens.* **2015**, *7*, 1021–1047. [[CrossRef](#)]
31. Thomas, A.C.; Reager, J.T.; Famiglietti, J.S.; Rodell, M. A GRACE-based water storage deficit approach for hydrological drought characterization. *Geophys. Res. Lett.* **2014**, *41*, 1537–1545. [[CrossRef](#)]
32. Long, D.; Scanlon, B.R.; Longuevergne, L.; Sun, A.Y.; Fernando, D.N.; Save, H. GRACE satellite monitoring of large depletion in water storage in response to the 2011 drought in Texas. *Geophys. Res. Lett.* **2013**, *40*, 3395–3401. [[CrossRef](#)]

33. Food and Agriculture Organization of the United Nations, Dams. Available online: <http://www.fao.org/nr/water/aquastat/dams/index.stm> (accessed on 9 January 2016).
34. Han, G.; Liu, C. Hydrogeochemistry of Wujiang river water in Guizhou province, China. *Chin. J. Geochem.* **2001**, *20*, 240–248. [[CrossRef](#)]
35. Zhang, M.; Wei, X.; Sun, P.; Liu, S. The effect of forest harvesting and climatic variability on runoff in a large watershed: The case study in the upper Minjiang River of Yangtze River basin. *J. Hydrol.* **2012**, *464*, 1–11. [[CrossRef](#)]
36. Chen, J.; Wilson, C.R.; Tapley, B.D. The 2009 exceptional Amazon flood and interannual terrestrial water storage change observed by GRACE. *Water Resour. Res.* **2010**, *46*. [[CrossRef](#)]
37. Wahr, J.; Molenaar, M.; Bryan, F. Time variability of the Earth's gravity field: Hydrological and oceanic effects and their possible detection using GRACE. *J. Geophys. Res.* **1998**, *103*, 30205–30229. [[CrossRef](#)]
38. Luo, Z.; Li, Q.; Zhang, K.; Wang, H. Trend of mass change in the Antarctic ice sheet recovered from the GRACE temporal gravity field. *Sci. China Earth Sci.* **2012**, *55*, 76–82. [[CrossRef](#)]
39. Cheng, M.; Tapley, B.D. Variations in the Earth's oblateness during the past 28 years. *J. Geophys. Res.* **2004**, *109*. [[CrossRef](#)]
40. Swenson, S.; Wahr, J. Post-processing removal of correlated errors in GRACE data. *Geophys. Res. Lett.* **2006**, *33*. [[CrossRef](#)]
41. Zhang, Z.Z.; Chao, B.F.; Lu, Y.; Hsu, H.T. An effective filtering for GRACE time-variable gravity: Fan filter. *Geophys. Res. Lett.* **2009**, *36*. [[CrossRef](#)]
42. Rodell, M.; Houser, P.; Jambor, U.E.A.; Gottschalck, J.; Mitchell, K.; Meng, C.; Arsenault, K.; Cosgrove, B.; Radakovich, J.; Bosilovich, M. The global land data assimilation system. *Bull. Am. Meteorol. Soc.* **2004**, *85*, 381–394. [[CrossRef](#)]
43. GRACE Tellus. Available online: <http://GRACEtellus.jpl.nasa.gov/> (accessed on 2 July 2015).
44. China Meteorological Administration. China Meteorological Data Sharing Service System. Available online: <http://cdc.nmic.cn/home.do> (accessed on 2 July 2015).
45. Morishita, Y.; Heki, K. Characteristic precipitation patterns of El Niño/La Niña in time-variable gravity fields by GRACE. *Earth Planet. Sci. Lett.* **2008**, *272*, 677–682. [[CrossRef](#)]
46. Linage, C.; Kim, H.; Famiglietti, J.S.; Yu, J.Y. Impact of Pacific and Atlantic sea surface temperatures on interannual and decadal variations of GRACE land water storage in tropical South America. *J. Geophys. Res.* **2013**, *118*, 10811–10829. [[CrossRef](#)]
47. Guo, Y.; Wang, J.; Zhao, Y. Numerical simulation of the 1999 Yangtze River valley heavy rainfall including sensitivity experiments with different SSTA. *Adv. Atmos. Sci.* **2004**, *21*, 23–33. [[CrossRef](#)]
48. Wang, Y.; Yan, Z. Changes of frequency of summer precipitation extremes over the Yangtze River in association with large-scale oceanic-atmospheric conditions. *Adv. Atmos. Sci.* **2011**, *28*, 1118–1128. [[CrossRef](#)]
49. Hu, K.; Huang, G.; Wu, R. A strengthened influence of ENSO on August high temperature extremes over the Southern Yangtze River Valley since the late 1980s. *J. Clim.* **2013**, *26*, 2205–2221. [[CrossRef](#)]
50. Tang, J.; Cheng, H.; Liu, L. Assessing the recent droughts in Southwestern China using satellite gravimetry. *Water Resour. Res.* **2014**, *50*, 3030–3038. [[CrossRef](#)]
51. Wang, B.; Zhang, Q. Pacific-East Asian teleconnection. Part II: How the Philippine Sea anomalous anticyclone is established during El Niño development. *J. Clim.* **2002**, *15*, 3252–3265. [[CrossRef](#)]
52. Saji, N.; Goswami, B.N.; Vinayachandran, P.; Yamagata, T. A dipole mode in the tropical Indian Ocean. *Nature* **1999**, *401*, 360–363. [[CrossRef](#)] [[PubMed](#)]
53. Ashok, K.; Guan, Z.; Saji, N.; Yamagata, T. Individual and combined influences of ENSO and the Indian Ocean dipole on the Indian summer monsoon. *J. Clim.* **2004**, *17*, 3141–3155. [[CrossRef](#)]
54. Meyers, G.; McIntosh, P.; Pigot, L.; Pook, M. The years of El Niño, La Niña, and interactions with the tropical Indian Ocean. *J. Clim.* **2007**, *20*, 2872–2880. [[CrossRef](#)]
55. Risbey, J.S.; Pook, M.J.; McIntosh, P.C.; Wheeler, M.C.; Hendon, H.H. On the remote drivers of rainfall variability in Australia. *Mon. Weather Rev.* **2009**, *137*, 3233–3253. [[CrossRef](#)]
56. Becker, R.; Sultan, M.; Becker, D. Effects of the Indian Ocean Temperature on Nile River Flow Volumes. In Proceedings of the American Geophysical Union Fall Meeting, Washington, DC, USA, 2009; Volume 1, p. 0262.
57. Sahu, N.; Behera, S.K.; Yamashiki, Y.; Takara, K.; Yamagata, T. IOD and ENSO impacts on the extreme stream-flows of Citarum river in Indonesia. *Clim. Dyn.* **2012**, *39*, 1673–1680. [[CrossRef](#)]

58. Ouyang, R.; Liu, W.; Fu, G.; Liu, C.; Hu, L.; Wang, H. Linkages between ENSO/PDO signals and precipitation, streamflow in China during the last 100 years. *Hydrol. Earth Syst. Sci.* **2014**, *18*, 3651–3661. [[CrossRef](#)]
59. Verdon, D.C.; Wyatt, A.M.; Kiem, A.S.; Franks, S.W. Multidecadal variability of rainfall and streamflow: Eastern Australia. *Water Resour. Res.* **2004**, *40*. [[CrossRef](#)]
60. Da Silva, G.A.M.; Drumond, A.; Ambrizzi, T. The impact of El Niño on South American summer climate during different phases of the Pacific Decadal Oscillation. *Theor. Appl. Clim.* **2011**, *106*, 307–319. [[CrossRef](#)]
61. Zhao, Q.; Wu, W.; Wu, Y. Variations in China’s terrestrial water storage over the past decade using GRACE data. *Geod. Geodyn.* **2015**, *6*, 187–193. [[CrossRef](#)]
62. Landerer, F.; Swenson, S. Accuracy of scaled GRACE terrestrial water storage estimates. *Water Resour. Res.* **2012**, *48*. [[CrossRef](#)]
63. Ministry of Water Resources, the People’s Republic of China. Available online: http://www.mwr.gov.cn/slxz/sjzsdwdt/201309/t20130910_512085.html (accessed on 21 April 2016).
64. Korecha, D.; Barnston, A.G. Predictability of June–September rainfall in Ethiopia. *Mon. Weather Rev.* **2007**, *135*, 628–650. [[CrossRef](#)]
65. Chakravorty, S.; Gnanaseelan, C.; Chowdary, J.; Luo, J.J. Relative role of El Niño and IOD forcing on the southern tropical Indian Ocean Rossby waves. *J. Geophys. Res.* **2014**, *119*, 5105–5122. [[CrossRef](#)]
66. Peterson, T.C.; Stott, P.A.; Herring, S. Explaining extreme events of 2011 from a climate perspective. *Bull. Am. Meteorol. Soc.* **2012**, *93*, 1041–1067. [[CrossRef](#)]
67. Chen, J.; Wen, Z.; Wu, R.; Chen, Z.; Zhao, P. Interdecadal changes in the relationship between Southern China winter-spring precipitation and ENSO. *Clim. Dyn.* **2014**, *43*, 1327–1338. [[CrossRef](#)]
68. Wu, R.; Yang, S.; Wen, Z.; Huang, G.; Hu, K. Interdecadal change in the relationship of southern China summer rainfall with tropical Indo-Pacific SST. *Theor. Appl. Clim.* **2012**, *108*, 119–133. [[CrossRef](#)]
69. Wu, G.; Zhang, Y. Tibetan Plateau forcing and the timing of South Asia monsoon and South China Sea monsoon. *Mon. Weather Rev.* **1998**, *126*, 913–927. [[CrossRef](#)]
70. Xu, M.; Chang, C.P.; Fu, C.; Qi, Y.; Robock, A.; Robinson, D.; Zhang, H.M. Steady decline of east Asian monsoon winds, 1969–2000: Evidence from direct ground measurements of wind speed. *J. Geophys. Res.* **2006**, *111*. [[CrossRef](#)]
71. Zhang, Q.; Xu, C.-Y.; Jiang, T.; Wu, Y. Possible influence of ENSO on annual maximum streamflow of the Yangtze River, China. *J. Hydrol.* **2007**, *333*, 265–274. [[CrossRef](#)]
72. Wang, L.; Chen, W.; Zhou, W.; Huang, G. Drought in southwest China: A review. *Atmos. Ocean. Sci. Lett.* **2015**, *10*. [[CrossRef](#)]
73. Lu, E.; Liu, S.; Luo, Y.; Zhao, W.; Li, H.; Chen, H.; Zeng, Y.; Liu, P.; Wang, X.; Higgins, R.W. The atmospheric anomalies associated with the drought over the Yangtze River basin during spring 2011. *J. Geophys. Res.* **2014**, *119*, 5881–5894. [[CrossRef](#)]



© 2016 by the authors; licensee MDPI, Basel, Switzerland. This article is an open access article distributed under the terms and conditions of the Creative Commons Attribution (CC-BY) license (<http://creativecommons.org/licenses/by/4.0/>).